Time–Temperature–Transformation Cure Diagrams of Phenol–Formaldehyde and Lignin–Phenol–Formaldehyde Novolac Resins

J. M. Pérez, F. Rodríguez, M. V. Alonso, M. Oliet

Department of Chemical Engineering, Faculty of Chemical Sciences, Complutense University of Madrid, Avda Complutense s/n, 28040 Madrid, Spain

Received 29 January 2010; accepted 25 May 2010
DOI 10.1002/app.32866
Published online 30 August 2010 in Wiley Online Library (wileyonlinelibrary.com).

ABSTRACT: In this study, the time–temperature–transformation (TTT) cure diagrams of the curing processes of several novolac resins were determined. Each diagram corresponded to a mixture of commercial phenol–formaldehyde novolac, lignin–phenol–formaldehyde novolac, and methylolated lignin–phenol–formaldehyde novolac resins with hexamethylenetetramine as a curing agent. Thermomechanical analysis and differential scanning calorimetry techniques were applied to study the resin gelation and the kinetics of the curing process to obtain the isoconversional curves. The temperature at which the material gelled and vitrified [the glass-transition temperature at the gel point ($_{gel}T_g$)], the glass-transition temperature of the uncured material (without crosslinking; T_{g0}), and the glass-transition temperature with full crosslinking were also obtained. On the basis of the measured of conversion degree at gelation, the approximate glass-transition temperature/conversion relationship, and the thermokinetic results of the curing process of the resins, TTT cure diagrams of the novolac samples were constructed. The TTT diagrams showed that the lignin–novolac and methylolated lignin–novolac resins presented lower T_{g0} and $_{gel}T_g$ values than the commercial resin. The TTT diagram is a suitable tool for understanding novolac resin behavior during the isothermal curing process. © 2010 Wiley Periodicals, Inc. J Appl Polym Sci 119: 2275–2282, 2011

Key words: curing of polymers; differential scanning calorimetry (DSC); resins

INTRODUCTION

Phenol–formaldehyde novolac resins (PFs) are widely used in industry because of their flame and chemical resistance, electrical insulation, and dimensional stability.[1] However, the high cost of phenol has increased the search for new alternatives in the formulation of phenolic resins. Thus, an alternative extensively studied is the utilization of natural compounds as fillers or extenders in the synthesis of PFs. One of the possible partial substitutes for phenol is lignin, which exhibits a structure close to a phenolic resin.[2] In addition, these natural compounds have also been modified to increase their reactivity toward formaldehyde during the polymerization reaction. More details have been provided elsewhere.[3–5] Although the formulation and the influence of variables (pH, catalyst, temperature, and so on) have been widely studied, the curing stages of novolac resins with natural fillers or extenders are unknown. However, this stage is crucial for determining the properties and quality of the material in its final application.

The time–temperature–transformation (TTT) diagram is a useful tool for designing thermosetting polymer curing cycles for final application. These diagrams show the phenomenological changes that occur during the process, such as gelation and vitrification and char and isoconversion contours, including the maximum conversion (α) curve. Gelation corresponds to the incipient formation of an infinite molecular network, which gives rise to long-range elastic behavior in a macroscopic fluid. This event occurs at a definite α for a given system according to Flory's theory of thermosetting polymer gelation.[6] After gelation, the material normally consists of miscible sol (solvent-soluble) and gel (solvent-insoluble) fractions, where the ratio of the former to the latter decreases with α. The gel point represents the state beyond which the material no longer flows and, therefore, cannot be processed. The material is liquid or rubbery when $T_{cure} > T_g$, where T_{cure} is the curing temperature and T_g is the glass-transition temperature. Vitrification is understood as a change in the liquid or rubbery state of resin due to an increase in both the crosslinking density and the molecular weight of the material during its curing process. This transformation takes place when T_g of the material coincides with T_{cure}.

Correspondence to: J. M. Pérez (jmperezr@quim.ucm.es).
Contract grant sponsor: Ministerio de Ciencia e Innovación; contract grant number: CTQ2007-64071/PPQ.

© 2010 Wiley Periodicals, Inc.

At this stage, resin curing within the glassy state becomes extremely slow, and the control over the overall process kinetics changes from a chemical reaction to a diffusion stage. Vitrification of the resin does not occur under isothermal curing if T_{cure} is above the glass-transition temperature of the fully cured resin ($T_{g\infty}$), that is, the highest T_g or the lowest temperature at which complete curing of the material can be achieved. At temperatures immediately above the glass-transition temperature of the uncured material (T_{g0}), its vitrification time (t_v) presents a maximum because of the opposite influence of the temperature on the resin viscosity and the reaction rate constant of the process. At higher temperatures, the time needed for polymer vitrification goes through a minimum as $T_{g\infty}$ is approached because of the opposite influences of the reaction rate constant and the decreasing concentration of reactants in the vitrification state.

Another parameter displayed in TTT diagrams is the glass-transition temperature at the gel point ($_{gel}T_g$), the lowest T_{cure} that allows the material to gel before it vitrifies, which coincides with T_{cure}, at which the material gels and vitrifies simultaneously. Below T_{g0}, the material does not crosslink. Between T_{g0} and $_{gel}T_g$, the liquid resins react until T_g attains the value of T_{cure}; at this moment, the vitrification of the resin begins, and the overall process kinetics become controlled by the diffusion stage. Between $_{gel}T_g$ and $T_{g\infty}$, the material gels, and then, the material vitrifies when $T_{cure} = T_g$. Above $T_{g\infty}$, the material is fully cured and remains in the rubbery state after its gelling.

Considerable effort has been devoted to developing the TTT cure diagrams of different polymers, such as epoxy systems, bisphenol A epoxy, epoxy–novolac resins, and phenolic resins.[7–10] In the literature, several techniques can be found for elaborating the TTT cure diagrams of thermosetting polymers. For instance, differential scanning calorimetry (DSC) is the most common technique for determining T_g and the curing degree of resins.[11–15] Thermomechanical analysis (TMA) and dynamic mechanical analysis (DMA) are techniques used for obtaining the gelation of the resin.[7,15–21]

In previous studies, we examined the formulation and curing kinetics for lignin–phenol–formaldehyde, methylolated lignin–phenol–formaldehyde, and commercial novolac resins.[22–24] In this study, we used the Flynn–Wall–Ozawa (FWO) isoconversional method to study the resins' curing kinetics on the basis of dynamic analysis by DSC.[25] The FWO method was applied to different α's of the cured resins. Having determined the kinetic data of the curing of the resins, we focused on the development of the TTT cure diagrams for a commercial PF and two lignin–phenol–formaldehyde novolac resins (LNs) in which phenol was partially substituted by ammonium lignosulfonate as an extender (methylolated) or filler (not methylolated) with 9 wt % hexamethylenetetramine (HMTA) as a curing agent; here, we used the DSC and TMA techniques were used. In addition, we also focused on the influence of the lignin type, methylolated or not, on the curing process of the novolac resins.

EXPERIMENTAL

Materials

A commercial PF (water content = 0.4 wt %, free phenol = 0.2%, flow distance = 25–40 mm) and HMTA were supplied by Hexion Specialty Chemicals Ibérica, S. A. (Guipúzcoa, Spain). The softwood ammonium lignosulfonate was supplied by Borregard Deutchland (Sapsborg, Norway) as Borresperse AM 320. The substitution of phenol by ammonium lignosulfonate was 30 wt % in both samples because higher amounts would not produce suitable resins.[26,27] The details of the modification of lignosulfonate were reported in a previous article.[5]

The formulations of the LN and methylolated lignin–phenol–formaldehyde novolac resins (MLNs) were carried out in a laboratory glass reactor equipped with a stirrer, thermometer, and reflux condenser. First, lignosulfonate (modified or unmodified), phenol, and oxalic acid (0.5 wt % in relation to phenol) were dissolved and heated to a temperature of 100°C. Then, the formaldehyde was added, and heating continued for 90 min. Second, a condensation reaction took place for 90 min. Afterward, the excess of nonreacted phenol and formaldehyde was removed. More details were provided in a previous article.[22] The three resins studied were cured with 9 wt % HMTA to obtain the thermosetting polymers.

Procedure and techniques

Calorimetric analysis was carried out with a Mettler-Toledo DSC 821^e. The weight of the novolac samples was around 4–6 mg. All of the samples were cured under a nitrogen atmosphere. All thermograms were normalized by calorimeter software to 1 g. Dynamic curing of the resins was carried out at nine heating rates (β's) of 2, 4, 6, 8, 10, 12, 14, 16, and 20°C/min from 30 to 250°C. Dynamic DSC runs made it possible to determine a kinetic model for both the curing of the resin samples and the iso-T_g relation. The data treatment of the dynamic curing processes by DSC began with a calculation of the curing degree of the resins by the following equation:

$$\alpha = \frac{(\Delta H_p)_t}{\Delta H_0} \quad (1)$$

where $(\Delta H_p)_t$ is the heat released up to time t and ΔH_0 is the total reaction heat associated with the

resin curing process, which is the average value of the total reaction heat obtained dynamically at different β values.

T_{g0} and $T_{g\infty}$ values were determined by dynamic DSC, with two sweeps performed at 10°C/min. The first sweep was performed from −20 to 250°C to determine T_{g0}. The second sweep was run from 0 to 250°C to obtain $T_{g\infty}$.[21,25,28]

Isothermal DSC was carried out for resins cured for different lengths of time at temperatures of 120, 140, 160, and 180°C to establish the relationship between the T_g of the polymer and the necessary curing time to attain a given α. The resins were not fully cured. As a result, it was necessary to quench them at −80°C to retain their polymerization state. They were scanned from −80 to 250°C at 10°C/min to obtain their T_g and residual heat. T_g was measured as the halfway point of the heat capacity, when the polymer consistency changed from the glassy to the rubbery state. In the case of the isothermal curing processes, the curing degree of the resins was calculated as follows:

$$\alpha = 1 - \frac{(\Delta H)_{t,\text{res}}}{\Delta H_0} \tag{2}$$

where $(\Delta H)_{t,\text{res}}$ is the residual heat obtained after isothermal curing up to time *t*.

A Mettler-Toledo TMA 840[e] analyzer was used to determine the change of resin from a viscous liquid to the solid state during its curing, a process known as *gelation*. This technique measures the length of the resin as a function of the temperature or time. The resin was placed between two silica disks 5 mm in diameter (ME-29595). The temperatures tested were 140, 150, 160, 170, and 180°C to reach the gel time. A periodic force (cycle time = 12 s) of 0.01 N was automatically applied to the resin sample. Because of this force, the probe moved up and down when the resin was still liquid. When the material reached gelation, the TMA measuring sensor was unable to respond to the force applied. At this moment, the sudden decrease in the amplitude of the oscillation revealed that the sample attained gelation. After the TMA process, the sample was cooled [temperature (T) = −4°C] and a dynamic DSC scan was performed at a β of 10°C/min to determine the residual heat and the gel conversion (α_{gel}) of the novolacs.

The methodology followed to develop the TTT cure diagrams of PF, LN, and MLN is shown in Figure 1. Thus, TMA and DSC assays were used to obtain the α at which the resins began to gel; DSC and the DiBenedetto equation were used to establish the vitrification points of the resins. ${}_{\text{gel}}T_g$ was determined by TMA and DSC. T_g, corresponding to a given α, was attained by isothermal DSC assays, and T_{g0} and $T_{g\infty}$ were determined with nonisothermal DSC runs.

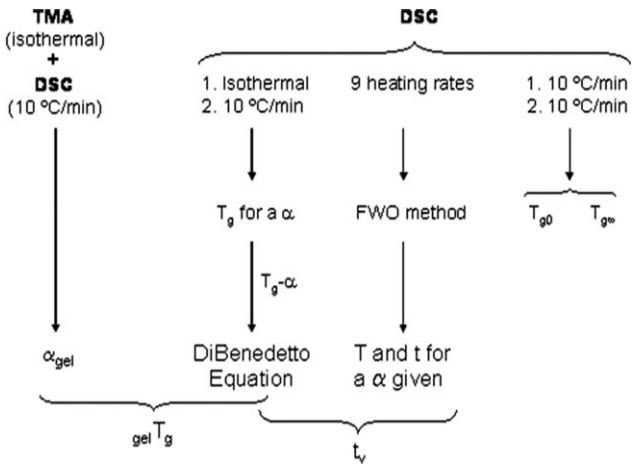

Figure 1 Scheme for the elaboration of TTT cure diagrams for thermosetting polymers.

Kinetic method

The isoconversional method used in this study was based on dynamic analysis by DSC. The reaction rate expression used to study the resins' curing kinetics can be expressed as follows:

$$\frac{d\alpha}{dt} = k(T) \times f(\alpha) \tag{3}$$

where $d\alpha/dt = \beta(d\alpha/dT)$, β is the heating rate (°C/min), $k(T)$ is the temperature-dependent rate constant, and $f(\alpha)$ is the function of the curing degree of the polymer. When one considers that the dependence on the temperature of the reaction rate constant of the resin curing process follows the Arrhenius expression, eq. (3) can be rewritten as

$$\beta\frac{d\alpha}{dT} = k_0 e^{(-E_a/RT)} f(a) \tag{4}$$

where T is the temperature (K), k_0 is the pre-exponential factor, E_a is the activation energy (kJ/mol), α is the resin curing degree, and R is the universal gas constant. Thus, the integral form of eq. (4) can be expressed as

$$g(\alpha) = \frac{k_0}{\beta}\int_0^{T_\alpha} e^{(-E_a/RT)}dT = \frac{k_0 E_a}{\beta R} P\left(\frac{E_a}{RT}\right) \tag{5}$$

where $g(\alpha) = \int_0^\alpha d\alpha/f(\alpha)$ is the integral form of the reaction model, T_α is the temperature corresponding to a specific degree of conversion. If $P\left(\frac{E_a}{RT}\right) = \int_\infty^0 \frac{e^{-E_a/RT}}{(E_a/RT)^2} dE_a/RT$ is assumed to be valid for an E_a/RT included between 60 and 20, eq. (5) is as follows:[29]

$$\log[P(E_a/RT)] = -2.315 - 0.456E_a/RT \tag{6}$$

TABLE I
Kinetic Parameters of Resin Curing Determined by the FWO Isoconversional Method

	9 wt % HMTA											
	PF				LN				MLN			
α	E_a (kJ/mol)	A	R^2	SD	E_a (kJ/mol)	A	R^2	SD	E_a (kJ/mol)	A	R^2	SD
2	136.4	18.185	0.988	0.052	95.9	14.821	0.932	0.124	97.4	15.119	0.897	0.151
10	125.9	17.277	0.994	0.037	92.5	13.977	0.980	0.068	96.2	14.462	0.979	0.069
20	122.8	16.772	0.995	0.033	92.4	13.753	0.989	0.049	91.9	13.585	0.988	0.052
30	121.3	16.515	0.995	0.032	93.8	13.803	0.993	0.040	91.4	13.352	0.992	0.043
40	120.3	16.331	0.996	0.032	95.4	13.918	0.995	0.033	92.0	13.301	0.994	0.037
50	119.5	16.179	0.995	0.033	96.7	14.000	0.996	0.029	92.6	13.289	0.995	0.033
60	118.7	16.033	0.995	0.034	97.2	13.981	0.996	0.029	93.0	13.253	0.996	0.031
70	118.1	15.892	0.994	0.036	96.9	13.858	0.996	0.030	92.9	13.170	0.996	0.030
80	117.4	15.738	0.993	0.042	96.1	13.673	0.996	0.031	92.2	12.994	0.996	0.031
90	116.6	15.527	0.988	0.053	94.9	13.401	0.995	0.035	90.1	12.628	0.995	0.033
95	115.5	15.282	0.983	0.062	94.2	13.216	0.993	0.039	88.7	12.361	0.995	0.035
99	110.0	14.432	0.974	0.077	93.8	13.011	0.992	0.044	87.3	12.041	0.994	0.037
100	93.7	12.204	0.973	0.079	86.8	11.914	0.998	0.024	83.7	11.383	0.993	0.039

$A = \log[k_0 E_a/g(\alpha)R] - 2.315$. SD = standard deviation.

To determine the kinetic parameters of the resin curing process, eqs. (4) and (5) can be combined and rearranged as follows:

$$\log \beta = A - 0.4567 \frac{E_a}{RT_\alpha} \tag{7}$$

where $A = \log[k_0 E_a/g(\alpha)R] - 2.315$. Equation (7) is known as the FWO isoconversional method,[30,31] which can be applied to different curing degrees of the resin.

RESULTS AND DISCUSSION

Curing kinetics

In the FWO isoconversional method, eq. (7) is applied to different α's of cured resins. According to this equation, for each α, the logarithm of β is correlated with the inverse of the temperature. For a given β, the temperatures at different curing degrees of novolac resins are obtained from the curves $\alpha - T$, as determined by dynamic DSC runs for each sample. The kinetic parameters of the curing process of LN, MLN, and PF obtained by the FWO method are shown in Table I and Figure 2. In most cases, the correlation coefficients (R^2's) were between 0.970 and 0.998. Data from Figure 2 show that the results of $\alpha = 2\%$ were the worst with respect to those of the remaining α values, especially in the case of LN and MLN. This behavior may have been due to the predominance of the thermal decomposition of resins on its cure at this low α. This fact is accentuated by the presence of lignin, modified or not, in the resin.

The tendency of the E_a values for MLN and PF with 9 wt % HMTA at a low curing degree ($\alpha \leq 20\%$) was to decrease from 97 to 90 kJ/mol for MLN and from 136 to 120 kJ/mol for PF. This was due to the formation of reaction intermediates, such as benzoazines and benzylamines, as a result of the incorporation of HMTA.[1] The E_a value for PF ($20 < \alpha \leq 90\%$) was over 119 kJ/mol, and that for MLN ($20 < \alpha \leq 80\%$) was over 92 kJ/mol. The E_a values did not change with the curing degree, which indicates that the reaction mechanism took place through parallel reactions. An abrupt decrease in the E_a values at the end of the curing process for MLN and PF occurred because the overall process kinetics were controlled by the diffusion stage.[32–34] The value of E_a for LN curing (92–97 kJ/mol) did not change significantly with temperature, including the anomalous data in the α range of 10–30%. This may have been because the overall process rate was governed by the diffusion stage.[35] This behavior only occurred with the LN cure because the unmodified lignin appeared to be poorly reactive.

T_g versus α relationship

The empirical DiBenedetto equation has been used in numerous studies; it provides a one-to-one relationship between T_g and α when the chemical structure of the resin is independent of the curing type.[7,36,37] This equation assumes that the resins reach full curing ($\alpha = 1$). Thus, the empirical DiBenedetto equation makes it possible to relate T_g to the α of the resin as follows:[7,14,16,17,20,38,39]

$$\frac{T_g - T_{g0}}{T_{g\infty} - T_{g0}} = \frac{\lambda\alpha}{1 - (1 - \lambda)\alpha} \tag{8}$$

where $T_{g\infty}$ is the maximum glass-transition temperature obtained experimentally for the fully cured material and the coefficient λ is defined as the ratio of the mobility of

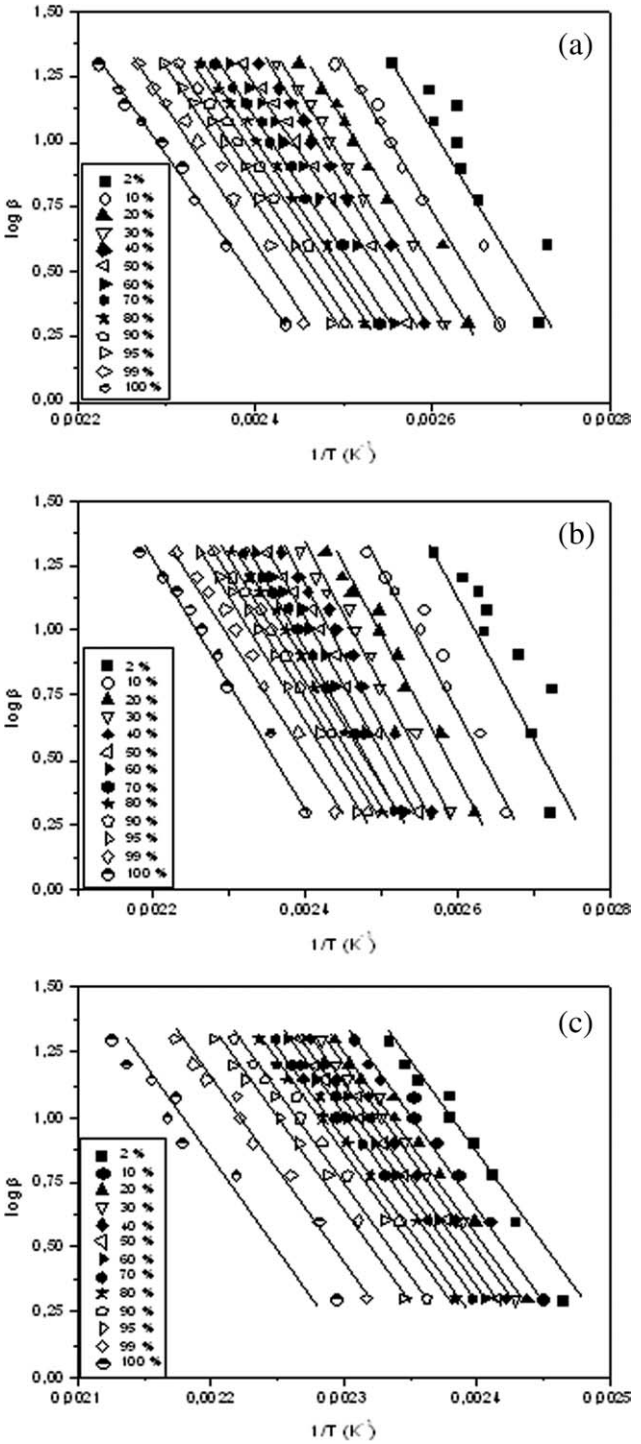

Figure 2 FWO relationship of log β versus $1/T$: (a) LN, (b) MLN, and (c) PF.

the segments between crosslinking nodes of the cured network at the end and at the start of the crosslinking process and is generally obtained experimentally from α and the three values of $T_{g\infty}$, T_g, and T_{g0}.

Each degree of resin curing presented a unique T_g, independent of T_{cure} and time conditions, as shown in Figure 3. Despite the dispersion of the T_g data at high α's, the existence of a relationship between T_g and α of the resin, which was independent of the isothermal cure temperature, was confirmed. This relationship was also observed by other authors.[7,14,36] This constitutes an important advance from the practical point of view because T_g can be measured more easily than α of resin. High α values cannot be measured by calorimetry because this technique does not detect changes in the residual heat.

The λ value is defined as the mobility relationship of the segments between the junction of networks

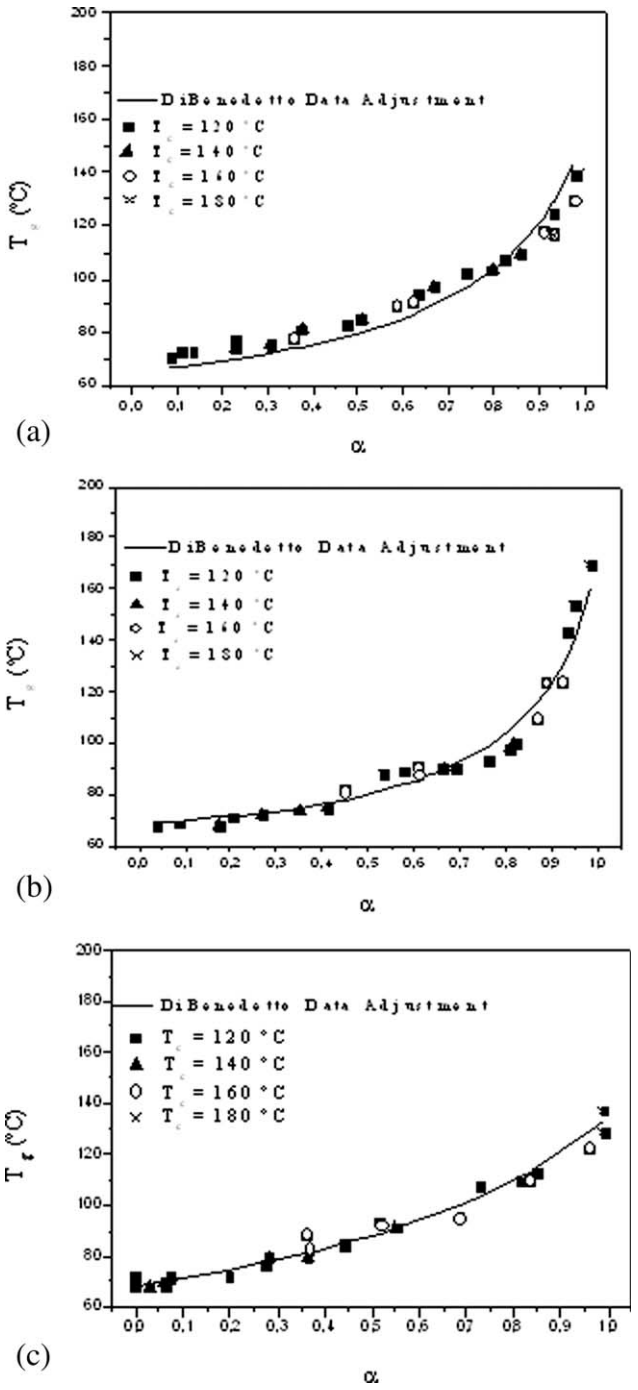

Figure 3 T_g versus α experimental data and DiBenedetto data fit: (a) LN, (b) MLN, and (c) PF.

TABLE II
Experimental Values of λ for Different Thermosetting Polymers Obtained by the DiBenedetto Equation

Resin	λ± Standard error	R^2
Lignin–novolac[a]	0.1993 ± 0.0194	0.959
Methylolated–lignin–novolac[a]	0.1316 ± 0.0091	0.892
Phenol–formaldehyde[a]	0.4089 ± 0.0279	0.970
Epoxy–diglycidyl ether of bisphenol A/1.2 diamine cyclohexane[7]	0.165	—
Epoxy–diglycidyl ether of bisphenol A/1.2 diamine cyclohexane/vinylcyclohexene dioxide[14]	0.349 ± 0.022	—
Epoxy–diglycidyl ether of bisphenol A/1.2 diamine cyclohexane/20% calcium carbonate[17]	0.501 ± 0.0128	0.984
Epoxy–diglycidyl ether of bisphenol A/methyl hexahydrophtalicanhydride/ benzyldimethylamine[20]	0.57	—
Epoxy system/TGDDM[36]	0.78	—
Epoxy–amine system[37]	0.44	—
Epoxy resin, commercial Hexcel 8551-7[38]	0.43 ± 0.04	—
Epoxy-based adhesive, commercial XS8436[39]	0.61613 ± 0.03637	0.934

An em dash indicates that the value is unknown.
TGDDM, Tetraglycidyl-4-4′-diaminodiphenylmethane.
[a] The sample was studied in this work.

crosslinking at the end and beginning of the resin's curing process.[11] Table II exhibits the λ values for PF, LN, and MLN with 9 wt % HMTA. In the literature, the λ values found varied from 0.17 to 0.78; this was in accordance with the resulted obtained for novolac samples.[7,14,17,20,36–39]

A higher λ value was obtained for PF curing in relation to LN and MLN curing. This fact, combined with the definition of the λ value, suggests that lignosulfonate incorporated into formulations as an extender or filler presented less mobility among its chains at the beginning and end of the curing process of the resins.

Gelation

Gelation is an important stage during the curing reaction of resins because from the gel point, the resin begins to flow with difficulty; this results in a high-molecular-weight polymer. In a previous study, the extent of the curing reaction at the gel point in relation to different T_{cure} values for PF, LN, and MLN with 9 wt % HMTA was shown to obey the isoconversional principle.[23] α_{gel} of the novolac resins changed with time; however, the α_{gel} value was independent of the T_{cure} used (Fig. 4). In the literature, we found that the resin α_{gel} is generally lower than other thermosetting polymers, such as epoxy–amine,[11,13,38,40] phenolic resol,[15] and epoxy resins.[14,39,41]

T_{g0} and $T_{g\infty}$, and ${}_{gel}T_g$ determination

T_{g0} and $T_{g\infty}$ are also necessary to determine the TTT cure diagrams of resins. T_{g0} values for LN, MLN, and PF are shown in Table III. From an industrial point of view, these temperatures indicate that all of the uncured resin samples could be stored at room temperature without reacting, which is useful because it makes it possible to prolong the material life and to reduce cost by eliminating cold storage. ${}_{gel}T_g$ is defined as the temperature at which the resin vitrifies and gels simultaneously. This value is obtained by extrapolation of the isoconversional line of α_{gel}. LN, MLN, and PF presented ${}_{gel}T_g$ values of 71.9, 73.7, and 88.5°C, respectively. This

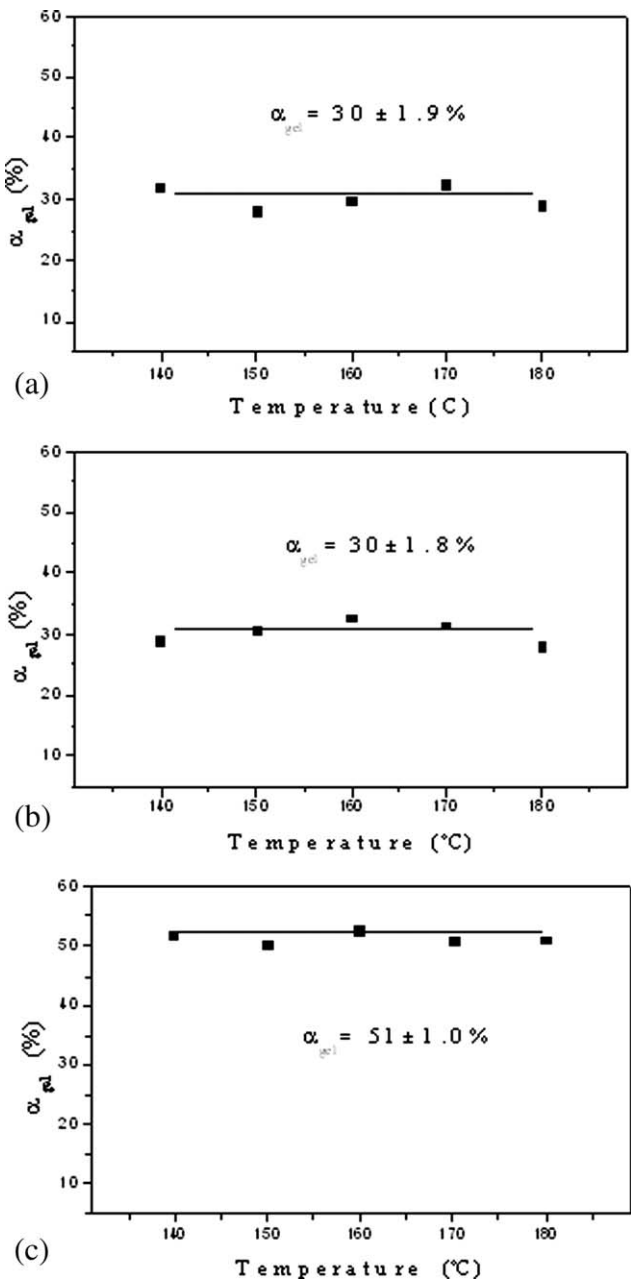

Figure 4 α_{gel} of each mixture from the resin and HMTA: (a) LN, (b) MLN, and (c) PF.

TABLE III
T_g Values Characteristic of the TTT Curing Diagrams for Different Thermosetting Polymers

Resin	T_{g0} (°C)	$_{gel}T_g$ (°C)	$T_{g\infty}$ (°C)
Lignin–novolac[a]	64.9	71.9	152.6
Methylolated lignin–novolac[a]	68.2	73.7	170.0
Phenol–formaldehyde novolac[a]	68.5	88.5	134.8
Epoxy–diglycidyl ether of bisphenol A/1.2 diamine cyclohexane[2]	−30.1	7.2	146.3
Diglycidyl ether of bisphenol F+ epoxy diluent[9]	−46.8	45.7	163.7
Epoxy–diglycidyl ether of bisphenol A/1.2 diamine cyclohexane/20% calcium carbonate[12]	−20.0	32.1	127.6
Tetrafunctional phenol novolac epoxy[13]	12	102	266
Anhydride-cured epoxy[15]	−40	4.5	150
Epoxy–novolac[35]	35	—	164
Phenol–formaldehyde resol[36]	−5.4	141	161
Methylolated lignin–phenolic resol[36]	−3.4	147.5	197
Powder coating[37]	60	68.5	75
Epoxy system[38]	−21.5	56.5	109

An em dash indicates that the value is unknown.
[a] The sample was studied in this work.

indicated a reduction of the mobility of the chains of LN and MLN during their curing, which was agreement with the respective λ values obtained.

The characteristic T_g values (T_{g0}, $_{gel}T_g$, and $T_{g\infty}$) for the elaboration of the TTT cure diagrams of the different thermosetting polymers are shown in Table III. Although each material presented a different TTT cure diagram because there were remarkable differences between them, the information supplied made it possible to optimize the curing conditions for thermosetting polymers for their final applications.

Vitrification points were calculated as the time needed for the polymer to reach the curing degree at which $T_g = T_{cure}$. The T_g values as a function of vitrification α and time are shown in Figures 5(a–c) for LN, MLN, and PF, respectively. LN and MLN needed more time to achieve vitrification; that is, these resin samples exhibited lower $_{gel}T_g$ and T_{g0} values with respect to the corresponding values of PF, but they exhibited higher T_g values. Therefore, novolac commercial resins needed higher temperatures than LN and MLN to avoid the vitrification stage during the curing process.

TTT cure diagrams

The different states through which the resin passes during its curing can be represented in a TTT cure diagram. For the construction of a TTT cure diagram, it is necessary to know the curing kinetics up to the point when the material vitrifies, the gel time, t_v, the isoconversional lines, the temperature of simultaneous gelation and vitrification, and the glass-transition temperature of resins without curing (T_{g0}) and that will full curing ($T_{g\infty}$). Therefore, TTT cure diagrams for the novolac systems were created with the experimental data determined in the foregoing sections. The values of k_0 and activation energy [E in eq. (9)] previously obtained for different curing degrees were fitted with an isoconversional expression such as

$$\ln t = k_0 + E/RT \tag{9}$$

This made it possible to obtain the isothermal T_g curves of the novolac resins (Fig. 5). The T_{g0} and $T_{g\infty}$ values were determined by DSC of the uncured and fully cured samples, respectively. The gelation line was drawn by the application of eq. (9). The t_v values were taken as the time required for the material to reach an α in which T_g was equal to T_{cure}. The temperature at which the material gelled and

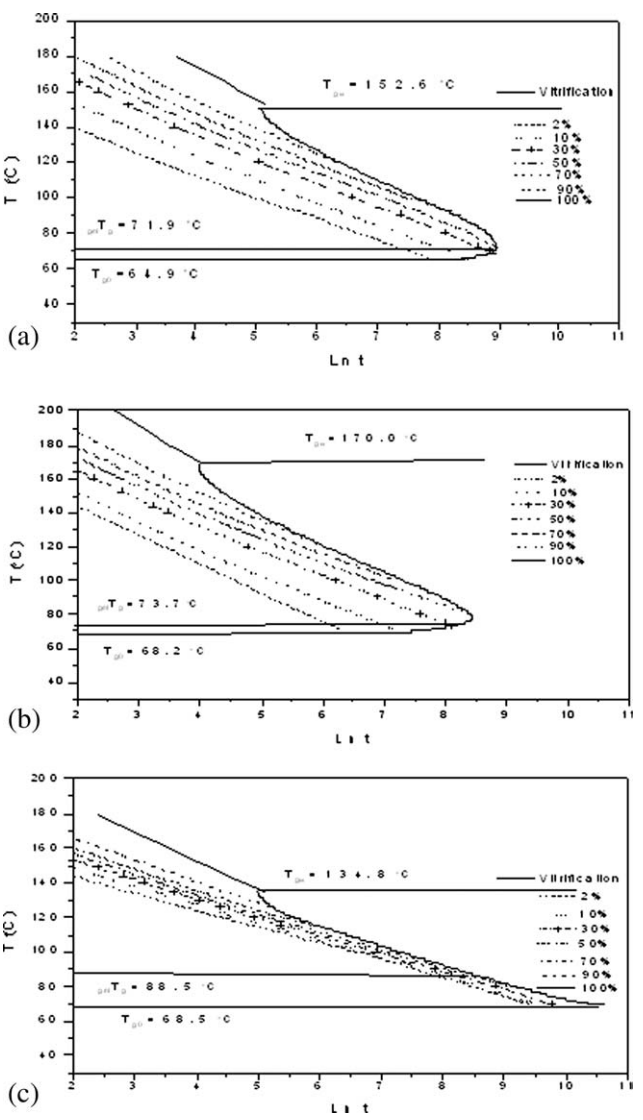

Figure 5 TTT cure diagrams for (a) LN, b) MLN, and (c) PF with 9 wt % HMTA.

vitrified simultaneously was ${}_{gel}T_g$. The time required for the material to gel and vitrify simultaneously was determined by the extrapolation of the isoconversional line of α_{gel} to a T_{cure} equal to ${}_{gel}T_g$.

The TTT cure diagrams for LN, MLN, and PF are shown in Figure 5. The ${}_{gel}T_g$ values were near T_{g0}, and in turn, the temperature was lower than the melting point. LN and MLN needed more time to finish their curing reactions in comparison to the PF. The cured PF gave a TTT diagram in which T_{g0} and $T_{g\infty}$ were closer to each other as compared with the same temperatures for LN and MLN.

The isoconversional lines for PF were also closer than those of LN and MLN. Thus, the LN and MLN isoconversional lines for $\alpha > 50\%$ showed that these resins needed more time to reach their full cure compared to PF. In the region where the resins were fully cured, the temperatures used to obtain the experimental data were close to those of thermal degradation. Therefore, when the cure reaction was above $T_{g\infty}$, a great amount of resin was thermally degraded, and the properties of the samples were lost. We also observed in the TTT cure diagrams that the vitrification line for all resins exhibited the typical sigmoidal profile (S-shape) of thermosetting polymers, with a minimum t_v.

CONCLUSIONS

In this study, we obtained three TTT diagrams by mixing a lignin–novolac, a methylolated lignin–novolac, and a commercial resin with a 9 wt % HMTA as a curing agent. As the results show, we concluded that the FWO isoconversional method can be applied to study the curing process kinetics of novolac and lignin–novolac polymers. Thus, the experimental results exhibited a dependence of the curing degree of LN, MLN, and PF on the E_a of the process. In addition, this method made it possible to obtain the data for the isothermal T_g curves for elaboration of the TTT cure diagrams for LN, MLN, and PF; the TTT cure diagram is a useful tool for designing the curing cycle of a resin for its final application.

The α_{gel} for all of the novolac resins assayed was independent of the temperature; this confirmed that the sample curing fulfilled the isoconversional principle. Both lignin–novolacs had similar α_{gel} values, and these were lower than that of the commercial resin. In this sense, the commercial resin showed a better curing process. In addition, LN and MLN exhibited lower ${}_{gel}T_g$ and T_{g0} values than the commercial resin but higher T_g values. Therefore, novolac resins needed higher temperatures than LN and MLN to avoid the vitrification stage during the curing process.

References

1. Gardziella, A.; Pilato, L. A.; Knop, A. Phenolic Resins. Chemistry, Applications, Standardization, Safety and Ecology, 2nd ed.; Springer-Verlag: Berlin, 2000.
2. Forss, K. G.; Furhmann, A. Forest Prod J 1979, 29(7), 39.
3. Alonso, M. V.; Oliet, M.; Rodríguez, F.; García, J.; Gilarranz, M. A.; Rodríguez, J. J. Biores Technol 2005, 96, 1013.
4. Alonso, M. V.; Oliet, M.; Rodríguez, F.; Astarloa, G.; Echeverría, J. M. J Appl Polym Sci 2004, 94, 643.
5. Alonso, M. V.; Rodríguez, J. J.; Oliet, M.; Rodríguez, F.; García, J.; Gilarranz, M. A. J Appl Polym Sci 2001, 82, 2661.
6. Flory, P. J. Principles of Polymer Chemistry; Cornell University Press: New York, 1953.
7. Núñez, L.; Fraga, F.; Castro, A.; Núñez, M. R.; Villanueva, M. Polymer 2001, 42, 3581.
8. Schiraldi, A.; Pezzati, E.; Baldini, P. Thermochim Acta 1987, 120, 315.
9. Lange, J.; Altmann, N.; Kelly, C. T.; Halley, P. J. Polymer 2000, 41, 5949.
10. Zhang, M. Z.; An, X.; Tang, B.; Yi, X. Front Mater Sci China 2007, 1(1), 81.
11. Wisanrakkit, G.; Gillham, J. K. J Appl Polym Sci 1990, 41, 2885.
12. Simon, S. L.; Gillham, J. K. J Appl Polym Sci 1992, 46, 1245.
13. Simon, S. L.; Gillham, J. K. J Appl Polym Sci 1994, 43, 709.
14. Núñez, L.; Villanueva, M.; Núñez, M. R.; Rial, B.; Fraga, L. J Appl Polym Sci 2004, 92, 1190.
15. Alonso, M. V.; Oliet, M.; García, J.; Rodríguez, F.; Echeverría, J. Chem Eng J 2006, 122, 159.
16. Pizzi, A.; Lu, X.; García, R. J Appl Polym Sci 1999, 7, 1915.
17. Núñez, L.; Taboada, J.; Fraga, L.; Núñez, M. R. J Appl Polym Sci 1997, 66, 1377.
18. Barral, L.; Cano, J.; López, J.; López-Bueno, I.; Nogueira, P.; Ramírez, C.; Torres, A.; Abad, M. J. J Them Anal Cal 1999, 56, 1025.
19. Pinoit, D.; Prud'homme, R. E. Polymer 2002, 43, 2321.
20. Teil, H.; Page, S. A.; Michaud, V.; Månson, J. A. E. J Appl Polym Sci 2004, 93, 1774.
21. Cadenato, A.; Salla, J. M.; Ramis, X.; Morancho, J. M.; Marroyo, L. M.; Martin, J. L. J Therm Anal 1997, 49, 269.
22. Pérez, J. M.; Rodríguez, F.; Alonso, M. V.; Oliet, M.; Echeverria, J. M. Bioresources 2007, 2, 270.
23. Pérez, J. M.; Oliet, M.; Alonso, M. V.; Rodriguez, F. Thermochim Acta 2009, 487, 39.
24. Pérez, J. M.; Rodriguez, F.; Alonso, M. V.; Oliet, M.; Dominguez, J. C. J Therm Anal Cal 2009, 97, 979.
25. Alonso, M. V.; Oliet, M.; García, J.; Rodríguez, F.; Echeverría, J. J App Polym Sci 2007, 103, 3362.
26. Ysbrandy, R. E.; Sanderson, R. D.; Gerischer, G. F. R. Holzforschung 1992, 46, 249.
27. Kharade, A. Y.; Kale, D. D. Eur Polym J 1998, 34, 201.
28. Ramis, X.; Cadenato, A.; Morancho, J. M.; Salla, J. M. Polymer 2003, 44, 2067.
29. Doyle, C. D. Nature 1965, 207, 290.
30. Ozawa, T. B Chem Soc Jpn 1965, 38(1), 1881.
31. Flynn, J. H.; Wall, L. A. J Res Natl Bur Stand Sect A 1966, 70, 487.
32. He, G.; Riedl, B.; Aït-Kadi, A. J Appl Polym Sci 2003, 89, 1371.
33. Wang, M.; Wei, L.; Zhao, T. Eur Polym J 2005, 41, 903.
34. Ren, S. P.; Lan, Y. X.; Zhen, Y. Q.; Ling, Y. D.; Lu, M. G. Themochim Acta 2005, 440, 60.
35. Vyazovkin, S. Thermochim Acta 1994, 236, 1.
36. Barral, L.; Cano, J.; López, J.; Nogueira, P.; Ramírez, C.; Abad, M. J. Polym Int 1997, 42, 301.
37. Perrin, F. X.; Nguyen, T. M. H.; Vernet, J. L. Eur Polym J 2007, 43, 5107.
38. Pascault, J. P.; Williams, R. J. J. J Polym Sci Part B: Polym Phys 1990, 28, 85.
39. Simon, S. L.; McKenna, G. B.; Sindt, O. J Appl Polym Sci 2000, 76, 495.
40. Enns, J. B.; Gillham, J. K. J Appl Polym Sci 1983, 28, 2567.
41. Yu, H.; Mhaisalkar, S. G.; Wong, E. H.; Khoo, G. Y. Thin Solid Films 2006, 504, 331.